Egypt. J. Chem. **Vol. 64**, No. 11. pp. 6251 – 6268 (2021)

Egyptian Journal of Chemistry

http://ejchem.journals.ekb.eg/

Evaluation of traditional, starch nanoparticle and its hybrid composite for the consolidation of tracing paper

Gomaa Abdel-Maksoud[a*], Rehab Khattab[b]

[a]*Conservation Department, Faculty of Archaeology, Cairo University, 12613 Giza, Egypt*

[b]*Conservation Center, National Archives of Egypt. Cairo, Egypt*

Abstract

Tracing paper was used since the 12th century. The deterioration of tracing paper occurs as a result of external factors (inappropriate environmental conditions), or internal factors (such as manufacture process). The manufacturing process plays a significant role in the deterioration process, since the preparation of tracing paper includes impregnating with oils or resins, heavy beating of the pulp, and treating the paper with chemicals such as sulfuric acid, and zinc chloride. The consolidation process is vital in the conservation of tracing paper to increase its strength and resistance against improper surrounding environmental conditions. Starch in its traditional form had been used as an adhesive for tracing paper since the last century. This paper aims to evaluate the use of starch in its traditional form and nanoscale form in improving the properties of 4 types of tracing paper. Mechanical properties, change of color, pH value, Fourier Transform Infrared spectroscopy (FTIR), and investigation of the surface morphology by scanning electron microscope (SEM) were used for the evaluation process. Thermal aging at 100 ^{o}C was used for the aging of treated and untreated tracing paper. The results revealed that the starch nanoparticles dissolved in water were the best consolidant for impregnated tracing paper. Starch nanoparticles with carboxymethyl cellulose dissolved in water were the best consolidant for the two types of genuine vegetable parchment paper. Starch nanoparticles dissolved in acetone with carboxymethyl cellulose were the best consolidant for modern tracing paper.

Keywords: Tracing paper, starch nanoparticle, consolidation, thermal ageing, deterioration, analytical techniques

1. Introduction

Historically, tracing paper is very important and had been used for different purposes. Medieval artists had used handmade tracing paper by impregnation technique in order to draw and copy their artworks as mentioned by Theophilus during the twelfth century, and by Cinnino during the middle of the fourteenth century. In the middle of the 19th century, there was an industrial revolution in the production of tracing paper. The French chemists Figuier and Poumarèze had taken in 1846 the first patent for chemically treated tracing paper (vegetable parchment paper). Then parchment paper was developed commercially by De La Rue Company in London based on a patent in 1857 by the chemist Gains **[1]**. At the end of the 19th century, the method of overbeaten tracing paper was used, which made it cheap and had high quality, and had become commonly used by artists, architects, geographers and engineers for writing and drawing. There is a large amount of artistic and other works executed on tracing paper in museums, storages, archives and libraries, which have different values (artistic, aesthetic, scientific, heritage, social and etc.) **[2-3]**.

Conservation of tracing papers is a complicated issue since tracing papers are produced by complex compositions and manufacturing processes giving three types of tracing papers. The first type of tracing paper is impregnated paper or vellum paper. Vellum paper has been manufactured by impregnating the paper with materials that have a similar index of refraction such as linseed oil, poppy-seed oil, starch, varnish, etc. This type of paper is performed on paper sheets made from rag pulp or chemical and mechanical wood pulp **[4-9]**. The second type is genuine vegetable parchment paper. From the middle of the nineteenth century, this paper has been transparentized by momentary immersion in baths of diminishing strengths of acid (such as sulfuric acid for thin paper or zinc chloride for thicker paper), and

*Corresponding author e-mail: gomaa2014@cu.edu.eg (Gomaa Abdel-Maksouda)

Receive Date: 15 May 2021, Revise Date: 27 May 2021, Accept Date: 06 June 2021

DOI: 10.21608/ejchem.2021.76272.3730

an alkaline neutralization bath follows the acid treatment. This method makes the paper translucent and similar to parchment. It is performed on paper sheets made mainly from cotton or/and linen pulp [7].later pure bleached wood pulp was used **[10- 13]**. The third type is paper from overbeaten fibers. At the end of the nineteenth century, cheaper alternatives to vegetable parchment were already being sought. It was discovered that a long beating of the paper fibers (i.e. chemical wood pulp) can also achieve the required transparency. These different types of tracing paper have various chemical and physical properties **[2-7]**, **[14]**.

Resultant tracing paper is mechanically weak due to the rough manufacturing procedures it goes through which results in paper with short fibers, as well as other factors such as frequent use, inappropriate housing, and improper conditions. Accordingly, tracing paper can strongly benefit from consolidation which increases its resistance to the surrounding environmental conditions. Since some types of tracing papers are extremely sensitive to moisture, the use of consolidants dissolved in an organic solvent is a better option compared to water-based consolidants **[4]**. The consolidation process for tracing paper aims to replace the lost sizing agent and improve the mechanical properties **[15]**. Many adhesives are conventionally used for treating tracing paper such as polyvinyl acetate **[16]**, sodium chloride of carboxymethyl cellulose **[17]**, starch **[18]**, gelatin, casein **[19]**, klucel G, and other cellulose ethers **[20]**.

In recent years, nanomaterials have also become vital for conservation treatment **[21]**. Starch nanoparticles (SNPs) can be produced by different methods such as enzymes, chemical, and physical treatments. The size distribution, crystalline structure, and physical properties of the SNPs may vary from one method to another **[22-24]**, starch nanoparticles is characterized by solubility in a common organic solvent such as acetone and toluene, which makes them suitable for consolidating tracing paper that are sensitive to water **[25]**.

Artificial accelerated aging is very necessary for evaluating the conservation process, especially for experimental studies. It assesses the changes in the properties of the used materials, and the evaluation of the used process **[26-27]**.

Analysis and investigation became vital in the conservation field in both experimental and applied studies. They detect the effectiveness of the evaluated materials by studying their properties. Mechanical properties such as tensile strength and elongation are very important to detect the ability of treated materials to improve their resistance against surrounding environmental conditions **[28]**. Color measurement is very necessary for evaluating the conservation materials **[29-30]**. The pH value measurement, FTIR, and investigation of the surface morphology by a scanning electron microscope are also important in experimental studies for the evaluation of conservation materials **[31-36]**.

This study aims to evaluate the effectiveness of the use of starch in different forms (i.e. in its traditional form dissolved in water, starch nanoparticles dissolved in water, or acetone, and mixture of starch nanoparticles dissolved in water, or acetone with carboxymethyl cellulose) in the consolidation of four modern types of tracing paper.

2. Materials and Methods

2.1. Materials and chemicals

- The types of tracing paper used in this study were impregnated paper or vellum paper, two types of Genuine vegetable parchment paper which were prepared by authors, and modern tracing paper (Rotring tracing paper) was purchased from Samir & Ali Library, Giza, Egypt.
- Natural starch (corn starch) and starch nanoparticles were purchased from the Nano Gate Company, Al Abageyah, El Mukkatam, Cairo, Egypt. Carboxymethyl cellulose (CMC), acetone and whatman paper were purchased from the AL Jumhuria Company for Chemicals, Cairo, Egypt.

2.2. Methods

2.2.1. Tracing paper samples preparation

2.2.1.1. Preparation of Impregnated paper or vellum paper:

Vellum paper was prepared according to Homburger and Korbel **[5]** by impregnating Whatman paper (high-quality cotton fibers) **[37]** in linseed oil. The paper was left to dry at room temperature. After impregnation, the color became dark yellow. The disappearance of dark yellow color is an indication of complete dryness. This type of paper was given the symbol (A).

2.2.1.2. Preparation of Genuine Vegetable Parchment Paper

Two types of genuine vegetable parchment paper were prepared as follow:

- Genuine vegetable parchment paper, given the symbol B, was prepared by momentary immersion in a bath of sulfuric acid 65% (v/v), followed by immersion in a neutralization bath (calcium hydroxide), which was repeated many times until the pH reached 7. This treatment made the paper translucent and similar to parchment **[1-3]**.
- Genuine vegetable parchment paper, given the symbol C, was prepared according to Jinxia et al. **[38]** by immersion in Zinc chloride dissolved in distilled water (60/40 v/w). The samples were pressed between two plastic sheets for five minutes. To maintain its moisture content, the treated paper was

rinsed with deionized water to extract the zinc chloride. Parchment paper has low transparency and is resistant to grease.

2.2.1.3. Modern tracing paper

Rotring tracing paper (overbeating fibers), given the symbol D, was purchased from Samir & Ali Library, Giza, Egypt.

2.2.2. Preparation of starch nanoparticles

Starch nanoparticles were purchased from Nano Gate Company which informed in its data sheet that the preparation process was according to Duan et al. **[39]**. 10 g of starch was dispersed in 1000 ml 3.16 M H_2SO_4 solution and stirred at 100 rad/min and a temperature 40°C for the desired time. The suspensions were then washed by successive centrifugations in water until the pH values were about 7.0. The final precipitate was freeze-dried to powder. The insoluble hydrolysis residues yield (wt%) were calculated by dividing the weight of freeze-dried precipitate by the initial dry weight of wax maize starch.The Company also provided the size and shape of starch nanoparticles. Transmission electron microscopy (TEM) was performed using a JEOL JEM-2100 high-resolution transmission electron microscope at an accelerating voltage of 200 kV (Fig. 1). The properties given by the company were: color: off-white; form: suspension; Avg. Size (TEM): 17±3 nm; and shape (TEM): spherical.

2.2.3. Preparation of Consolidants and the application method used for the treatment of tracing paper

Consolidants used are as follows:

- Starch in its natural form dissolved in distilled water (3%) by heating.
- Starch nanoparticles dissolved in water (3%)
- Starch nanoparticles dissolved in acetone (3%).
- Starch nanoparticles (3%) blending with Carboxymethyl Cellulose dissolved in distilled water (3%) (1:1 W/W).
- Starch nanoparticles dissolved in acetone (3%) blending with Carboxymethyl Cellulose (CMC) dissolved in water (3%) (1:1 W/W).

The sample numbers and applied treatments are described in Table 1.

It should be noticed that the authors preferred to use a mixture from starch nanoparticles with carboxymethyl to improve some properties of tracing paper. Ghanbarzadeh et al. **[40]**, Tongdeesoontorn et al. **[41]**, and Qiao et al**. [42]** proved that the blending of CMC with starch adhesive improved the viscosity, and increased the mechanical properties. The Improvement in mechanical properties that have occurred was due to interaction between the carboxyl group of CMC and the hydroxyl group of starch by replacing hydrogen bonds between starch molecules by hydrogen bonds formed between the hydroxyl groups in starch molecules and the hydroxyl and carboxyl groups in CMC. Mandal and Chakrabarty **[43]**, and Jannatyhaa et al. **[44]** proved that the blending of CMC with nanocellulose had the same effect. Accordingly, the authors found that it was necessary to study and evaluate the blending of CMC with starch nanoparticles to determine its ability for the improvement of some properties studied of tracing paper.

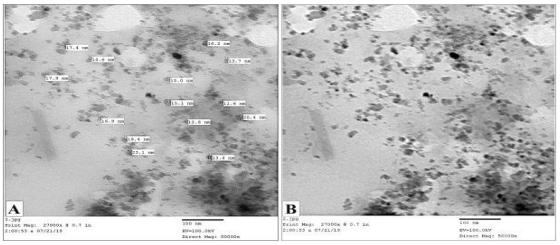

Fig. 1. (A, B) TEM images of the prepared Starch nanoparticles using two different magnifications from the images, it is obvious that, the nanoparticles were spherical and well dispersed, with an average size of about 17±3 nm (Nano Gate Company - Data Sheet).

The tested consolidants were applied to the paper samples using a soft brush. Excess consolidants was removed by covering the samples with a layer of Reemay and applying pressure on it using a ruler, starting from the middle to the out layer of the samples.

2.2.4. Artificial accelerated thermal aging:

Accelerated thermal aging was carried out on all samples at 100°C in a dry oven for 72 hours, according to U.S. Federal Specifications for Tracing Paper (No. UU-P-561H 1972) **[4]**. The procedure was carried out in nÜve - FN 500 oven at the Conservation Center, The National Archives of Egypt.

Table 1

Sample numbers and applied treatments

Sample No.	Treatment
C.S.	Control sample (Untreated)
1. (A,B,C,D)	Natural starch
2. (A,B,C,D)	Starch nanoparticles (SNPs) 3% dissolved in water
3. (A,B,C,D)	(SNPs) 3% dissolved in acetone
4. (A,B,C,D)	(SNPs) 3% + CMC 3% dissolved in distilled water.
5. (A,B,C,D)	(SNPs) 3% dissolved in acetone + CMC 3% dissolved in distilled water.

2.2.5. Analysis and investigation techniques

2.2.5.1. Tensile strength and elongation

Tensile strength and elongation were studied using the dynamometer produced by SDL ATLAS, H5KT. The samples were cut into strips about 2 cm × 10 cm. All measurements were made before and after aging. All measurements were applied at temperature of 20◦ C, relative humidity 65%. The load range was100 N, the extension range was 10 mm, the gauge length was 100 mm, and the speed was 100mm /min. The procedure was carried out at the National Institute of Standards (NIS), Giza, Egypt.

2.2.5.2. Color Change Measurements:

The color of the samples was measured using Optimatch 3100 ® from the SDL Company. The colors that are given in CIE- Lab coordinates are, the L value corresponding to the brightness (100 = white, and 0 = black), while a* value to the red-green coordinate (positive sign = red, and negative sign = green), and b* value of the yellow-blue coordinate (positive sign = yellow, and negative sign = blue). The total difference of color ΔE* between two color stimuli $\Delta E^* = \{(\Delta L^*)^2 + (\Delta a^*)^2 + (\Delta b^*)^2\}^{1/2}$ **[45]**, if ΔE* is less than 3, this means that the color change is not noticeable to the naked eye **[46]**. All samples were measured in a visible region. The procedure was carried at the National Institute of Standards (NIS) in Cairo, Egypt.

2.2.5.3. The pH value:

The pH values were measured using Lutron pH meter model PH- 211. The pH meter was calibrated with known buffer solutions (i.e. buffers of pH 7 and 4 pH are usually selected). The electrodes of the pH meter were rinsed with distilled water and then immersed in the buffer **[47-48]**. The pH measurement was done according to May and Jones **[49]** by soaking the paper in pure water and then measuring the pH of the aqueous extract. 2 g of paper were soaked in 100 ml water for 1 hour **[50]**. The procedure was carried out at the Conservation Center, The National Archives of Egypt.

2.2.5.4. Fourier Transform Infrared Spectroscopy (ATR-FTIR):

FTIR spectroscopy was used to study the functional groups in the paper samples and the change that have occurred due to treatments compared to the control sample to rate the chemical change **[51]**. ATR-FTIR spectra of paper samples were obtained using a Nicolet 380 FT-IR Spectrometer with ATR Crystal, in the frequency range of 4000 - 400 cm-1, in reflectance mode. The procedure was carried out at the National Institute of Standards (NIS), Cairo, Egypt.

2.2.5.5. Investigation of the surface morphology by Scanning Electron Microscopy (SEM)

Scanning electron microscopy was used to investigate the surface morphology of the treated samples. The samples were coated with gold. The samples were scanned using (JEOL JSM S400LV EDX Lin1 ISIS-Oxford high vacuum) at the Faculty of Science, Assiut University, Egypt. The investigation was performed on two treated paper, which gave the best results in terms of the other tested properties.

3. Results and Discussion

3.1. Tensile strength and Elongation:

The tensile strength and elongation results for all untreated samples (Table 2) decreased after aging. The reduction in tensile strength post aging was 26%, 30%, 29%, and 25% and in elongation was 20%, 30%, 26%, and 27%, for all types of paper (A, B, C, and D), respectively. These results were confirmed by Shahani **[52]**, Considine et al. **[53]**, Zhu et al. **[54]**. The decrease in tensile strength of untreated aged samples has been explained by Chapdelaine and Arney **[55]**, Zou et al. **[56]**, Whitmore et al. **[57]**, and Barański et al. **[58]**, who reported that the oxidation of cellulose caused weakening of the cellulose chain at the site of the oxidized groups (i.e. carboxylic groups) as a result of the loss of the water molecule of the bond C-OH in C2-C3 in the glucopyranose ring. The loss of fiber strength is due to re-polymerization and increased acidity following oxidation of the cellulose by the formation of carboxylic groups as a result of an oxidation process.

As for the consolidated samples (Table 2), the reduction in tensile strength for all consolidated paper samples post aging was less compared to the untreated aged samples. The reduction percentages for samples treated with starch dissolved in water, SNPs dissolved in water, SNPs dissolved in acetone, SNPs dissolved in water blending with CMC and SNPs dissolved in acetone blending with CMC, respectively, were 23%, 15%, 16%, 20% and 22% for paper type A; 20%, 21%, 24%, 25% and 27% for the paper B; 25%, 22%, 24%, 20% and 27% for paper C, and 23%, 22%, 19%, 21% and 17% for paper type D.

As for the reduction in elongation in aged samples previously treated with consolidants, it was less than the untreated aged paper (Table 2). The reduction percentages for samples treated with starch dissolved in water, SNPs dissolved in water, SNPs dissolved in acetone, SNPs dissolved in water blending with of CMC and SNPs dissolved in acetone blending with CMC, respectively, were 12%, 13%, 7%, 14% and 17 for paper type A; 17%, 18%, 23%, 24% and 21% for paper type B; 14%, 15%, 17%, 18% and 20% for

paper type C; 16%, 17%, 18%, 20, and 21% for paper type D.

The results proved that starch nanoparticles dissolved in water for paper type (A), starch nanoparticles dissolved in water blending with CMC for paper B and C, and starch nanoparticles dissolved in acetone for paper D are the most efficient compared to the other tested consolidants. These results were confirmed by Lin et al. **[25]**, Chandra et al. **[59]**, Dufresne **[60]**, Liu et al. **[61]**, Sandhu and Nian **[62]**, Huicochea and Rendon **[63]**, who stated that the starch nanoparticles network resulted from strong interactions between crystals by hydrogen bonds, which improve the mechanical properties, thermal properties, barrier properties, and also improve interfacial adhesion between starch nanoparticles and polymer matrices (cellulose of paper). The high specific surface area resulting from their nanoscale dimensions coupled with the high density of surface hydroxyl groups allows a strong bond with cellulose fibers in the paper.

3.2. Color Measurement

The results obtained (Table 3) show color values (L*, a*, and b*) and total color differences (ΔE). The results can be explained as follow:

3.2.1. Color values

Table 2

Measurement of tensile strength (maximum force/N) and elongation (%) of tracing paper (A, B, C and D) treated with consolidants before and after accelerated heat ageing

	Tensile strength (maximum force/N)							
	Paper A		Paper B		Paper C		Paper D	
C.	B.A.	A. A.	B.A.	A.A.	B.A.	A. A.	B. A.	A. A.
C.S.	29.93	22.20	25.15	17.72	24.9	17.80	69.80	52.20
1	39.20	30.01	54.20	43.50	59.6	44.80	87.86	67.20
2	35.70	30.30	31.89	25.24	55.3	43.24	82.10	64.40
3	34.89	29.28	29.55	22.24	40.2	30.44	85.30	69.20
4	27.80	22.30	94.50	69.15	69.6	55.58	80.40	63.50
5	31.04	24.10	85.20	64.20	52.6	38.54	76.60	63.34
	Elongation (%)							
C.S.	1.371	1.100	1.976	1.389	1.681	1.247	1.960	1.447
1	1.212	1.070	2.752	2.290	2.458	2.114	2.986	2.514
2	1.224	1.059	1.401	1.154	1.906	1.611	2.412	2.011
3	1.187	1.094	2.091	1.620	2.152	1.780	2.516	2.070
4	1.526	1.306	2.462	1.870	2.919	2.390	2.198	1.762
5	1.962	1.625	2.204	1.750	2.89	2.298	2.515	1.976

C. = Consolidants, B. A. = Before ageing, A.A. = After ageing

3.2.1.1. Lightness (L*)

It was clear from the obtained data (Table 3) that the L* value of the impregnated paper samples treated with different consolidants decreased in lightness compared to the control sample. The best results were obtained in the case of sample No. 3A, followed by samples No. 4A, 2A, 5A, and 1A, respectively. The results also indicated that the sample treated with starch nanoparticles gave better results than the sample treated with starch in the normal phase. The treated sample showed resistance against thermal aging compared to the control sample. The results also showed the effect of aging on the lightness of the untreated sample with a loss percentage of 5%. Results also revealed the capability of some consolidants (i.e. samples No. 3A, 1A, and 2A respectively) in protecting impregnated paper (A) from lightness decline compared to the control sample.

The lowest decrease in lightness was obtained in the case of samples No. 5A and 4A, respectively.

For vegetable parchment paper (B), the results revealed (Table 3) that all the aged samples treated with different consolidants decreased in lightness compared to the control sample.

The best results were obtained in the case of sample No. 2B, followed by samples No. 1B, 3B, 5B, and 4B, respectively. After aging, the treated samples gave resistance to thermal aging compared to the untreated sample. The highest resistance was obtained in sample No. 1B, followed by samples No. 3B, 2B, 4B, and 5B, respectively.

For vegetable parchment paper (C) (Table 3), before thermal aging, the results proved that all samples treated with different consolidants decreased in lightness compared to the control sample. The aged untreated and treated samples decreased in lightness post aging. The most resistant sample to thermal aging was sample No. 1C, followed by samples No. 2C, 3C, 5C, and 4C, respectively.

For modern paper (D) (Table 3), the results proved that the lightness of the treated sample before aging increased compared to the control sample. The highest increase in lightness was observed in sample No. 2D, followed by samples No. 3D, 1D, 5D, and 4D, respectively. The same observation was approximately obtained after thermal aging.

The samples treated with separate consolidants gave higher lightness values compared to the samples treated with composite consolidants, both before and after accelerated thermal aging; this may be due to the high viscosity of composite consolidants which reflects the color of the treated sample.

These results were confirmed by Zervos **[64]**, Ardelean et al. **[65]**, Karlovits and Gregor-Svetec **[66]**, who reported that the lightness of untreated and treated samples with studied consolidants decreased before and after thermal aging.

3.2.1.2. Red-green value (a*)

The a* values of the untreated and treated impregnated paper before aging (Table 3) indicate the color green. All the treated samples before aging, increased in green color compared to the control sample except the sample No. 4D. The treated samples after thermal aging revealed that the green color decreased for the samples 1A, 2A, and 3A compared to the control sample. The color of the sample No. 4A and 5A shifted to a red color, which indicate the effect of thermal aging on these samples.

For the treated genuine vegetable parchment paper (B), the a* value indicate a green color before and after thermal aging. The green color of treated samples after aging was less than before aging.

For the treated vegetable parchment paper (C), the a* value indicate a green color before and after accelerated thermal aging. Samples No. 1C, 2C, and 3 C were affected by thermal aging more than samples No. 4 and 5.

For the treated modern tracing paper (D), the a* value indicate a green color before and after thermal aging. The green color of the aged treated samples was less than the treated samples before aging.

3.2.1.3. Yellow-blue value (b*)

The results obtained (Table 3) showed that the treated impregnated paper (A) samples before aging were yellow. The treated samples increased in yellow color compared to the control sample except for the sample No.1A. For aged samples, the yellow color increased for all untreated and treated samples. The highest increase in yellow color after aging was obtained in the case of samples No. 5A followed by samples No. 4A, 1A, 2A, and 3A, respectively.

For the treated vegetable parchment paper (B), the yellow color of the treated sample before aging decreased compared to the control sample. The yellow color of the aged treated samples increased in most of the treated samples.

For the treated vegetable parchment paper (C), the yellow color of the treated samples before and after accelerated thermal aging increased compared to the control sample; however, the increase in yellow color is after aging.

For the treated of tracing paper (D), the yellow color increased before and after thermal aging compared to the control sample. It was also noticed that the yellow color of the aged treated samples was higher than the treated samples before aging.

Gonçalves et al. **[67**] stated that the use of acid in the preparation of starch nanoparticles gives a significant increase in a* and b* values. This observation was noticed in the samples treated with starch nanoparticles dissolved in water or acetone (2A, 3A) compared to the sample treated with starch in its normal form (1A). The increase in the b* value was found in the sample treated with carboxymethyl cellulose after aging. Asl et al. **[68]**, and Rosenau et al. **[69]** said that the paper samples treated with carboxymethyl cellulose tend to be in yellow after aging.

3.2.2. Total color differences (ΔE)

The total color differences (Table 3) of the treated impregnated paper (A) samples before aging was very similar for all consolidants used. The lowest change was obtained in the case of sample No. 1A (2.01) and the highest change was obtained in sample 3A (2.69). The lowest and highest changes in ΔE* were less than 3, which is not observable by the naked eye as was stated by Szucs and Lanyi **[46]**. After aging, the change in the total color was clear in the treated samples with starch nanoparticles dissolved in water + carboxymethyl cellulose, and the sample treated with starch nanoparticles dissolved in acetone + carboxymethyl cellulose (i.e. the ΔE value increased more than 5). The results of ΔE* for other samples were less than 3.

For the treated vegetable parchment paper (B), the change in ΔE* before and after accelerated thermal aging was less than 3 except for the samples No 5B, since its value was 3.56 before aging and 6.14 after aging.

For all the treated vegetable parchment paper (C) samples, ΔE* value was less than 3 before and after thermal aging.

For the treated modern tracing paper (D), the changes in ΔE* before aging was less than 3 for all samples, but the changes after aging were higher than 5 in samples No. 1D, 2D, and 3D. The value of ΔE* the samples No. 4D and 5D was less than 3.

3.3. The pH Values

The results (Table 4) showed that the pH values of all the control samples in different tracing paper decreased slightly after thermal aging except for paper B which has a good resistance against aging; this may due to the residue of calcium hydroxide used during the paper preparation which gave a future resistance against acidity. The results revealed that the pH of the treated paper decreased slightly after thermal aging except for the samples treated with starch in normal form, the sample treated with starch nanoparticles dissolved in water blending with carboxymethyl cellulose, and the sample treated with starch nanoparticles dissolved in acetone blending with carboxymethyl cellulose. Ardelean **[70]** confirmed that carboxymethyl cellulose leads to give a high contribution to alkalinity. It was noticed that the carboxymethyl cellulose gave more resistance against aging compared to other samples treated with other consolidants.

The results (Table 4) proved that the pH values of all samples decreased slightly after aging. Some authors **[37, 64]**, **[71-72]** explained that this may be due to the occurrence of oxidation of cellulose during thermally accelerated aging by the action of oxygen (autoxidation). Cellulose thermal degradation is expected to cause, the scission of chemical bonds between monomeric glucose units. Accordingly, decrease in its degree of polymerization with the formation of free radicals and carbonyl (i.e. carboxyl, aldehyde, and ketone). The oxidation of cellulose also contributes to raising the concentration of acid in the paper.

3.4. FTIR spectroscopy:

The results obtained (Fig. 2 A and B) for the paper samples A treated with different polymers before and after aging compared to the control sample were as follow:

The unaged control sample (Fig. 2 A) of paper (A) showed the presence of the following band which are characteristic of cellulose: the O-H stretching broad band appeared at 3334 cm^{-1} (its intensity 90.9) is characteristic for stretching vibration of the hydroxyl group in polysaccharides. This band includes inter- and intra-molecular hydrogen bond vibrations in cellulose, the C-H stretching vibration band of hydrocarbon constituent in polysaccharides at 2910 cm^{-1} and 2850 cm^{-1} (intensity 93.5 and 93.9, respectively), the C=O unconjugated band at 1739 cm^{-1} (intensity 91.9), the C=O conjugated and H-O-H correspond to vibration of water molecules absorbed in cellulose at 1624 cm^{-1} (intensity 96.6), the CH_2-COH is associated with the amount of the crystalline structure of cellulose at 1428 cm^{-1} (intensity 92.0) and C-O of cellulose polymerization at 1160, 1108, 1053 and 1029 cm^{-1} (intensities 84, 80, 72, 72, respectively) **[73-76]**. Post aging, the control sample (Fig. 2 B) showed a slight increase in the intensity of the O-H stretching band (approximately 1.6); this indicates that occurrence of a slight hydrolysis. The hydrolysis is indicated by cleavage of the hemiacetal bond between the two glucopyranose rings C1 and C4. The terminal rings resulting in the splitting of C1-O-C5 bond in the same ring **[77-79]**. There was an increase in the intensity of the C-O band; and this is mostly due to re-polymerization as a result of thermal aging. The thermal degradation caused the scission of glucosidic linkages of cellulose, and change degree of polymerization **[80-81]**.

Before aging, the samples treated with the studied consolidants (Fig. 2A) (starch, SNPs dissolved in water, SNPs dissolved in acetone, SNPs dissolved in water blending with CMC, and SNPs dissolved in acetone blending with CMC showed an increase in the intensities of the bands of the functional groups of the studied consolidants and a slight decrease in the C-O band at 1159-1001 cm^{-1} (i.e. cellulose polymerization). All these changes are due to the presence of the functional groups of starch, starch nanoparticles, and CMC after treatment **[82-91]**. Post aging, samples treated with all studied consolidants (Fig. 2B) showed a decrease in the intensities of the O-H stretching band, the C=O conjugated band, and the H-OH band. This may be due to the loss of water molecules as mentioned by Gorassini et al., Traore and Kaal **[92-93]**. The sample treated with SNPs dissolved in acetone showed an increase in the intensity of the C=O unconjugated band (the ester group) at 1741 cm^{-1} was noticed **[86]**. The sample treated with starch and SNPs dissolved in acetone blending with CMC showed a decrease in the intensity of the CH_2-COH absorption band at 1430 cm^{-1} associated with the amount of the crystalline structure of cellulose. The samples treated with SNPs dissolved in water and SNPs dissolved in acetone blending with CMC showed a decrease in the intensities of all C-O bands (cellulose polymerization bands); this may be due to the scission of glucosidic

linkages of cellulose. Accordingly, decrease degree of polymerization **[94]**.

The results obtained (Fig. 2C and D) for the treated paper samples B before and after aging were as follow:

Before aging, the control sample of paper B (Fig. 2C) showed the presence of the OH stretching broad band at 3340 cm^{-1} (intensity 96.0), C-H stretching band at 2903 cm^{-1} and 2858 cm^{-1} (intensity 98.3 and 98.6, respectively), C=O unconjugated band at 1740 cm^{-1} (intensity 96.9), C=O conjugated band and H-O-H band at 1637 cm^{-1} (intensity 98.7), CH_2-COH band of cellulose crystallization at 1425 cm^{-1} (intensity 97.4) and C-O of cellulose polymerization at 1160, 1109, 1055 and 1030 cm^{-1} (intensities 94, 91, 87, 86, respectively). The control sample after aging (Fig. 2D) showed a slight increase in the intensity of the O-H stretching band, which may be due to the occurrence of a slight hydrolysis. An increase in the intensities of the C=O unconjugated and H-O-H band were also noticed which occurred as a result of cellulose oxidation as mentioned by Chapdelaine and Arney **[55]**, Zou et al. **[56]**, Whitmore et al. **[57]**, Barański et al. [58], Ferrer and Sistach **[95]**, Lojewski et al. **[96]**, Librando and Minniti **[97]** reported that the oxidation of cellulose caused weakening of the cellulose chain at the site of the oxidized groups (carboxylic groups) as a result of the loss of the water molecule of the bond C-OH in C2-C3 in the glucopyranose ring. The increase in the intensities of CH_2-COH band is associated with the increase of amount of the crystalline structure of cellulose; while the increase in the C-O absorption bands of cellulose polymerization is due to due to change in the polymerization as a result of thermal aging. All treated samples showed an increase in the intensities of the bands of functional groups of consolidants studied; however, a decrease in the intensity of C-O band of cellulose polymerization was noticed in the samples treated with starch, SNPs dissolved in acetone, and SNPs dissolved in water blending with CMC. All treated samples after aging (Fig. 2D) showed a decrease in the intensities of the O-H stretching band, the C=O conjugated band, and the H-OH band, which may be due to the loss of water molecules. A decrease in the intensity of the CH_2-COH band of cellulose crystallization was observed in all treated samples and changes in the intensity of C-O at the also noticed as a result of thermal aging.

The results obtained (Fig. 2E and F) for the treated paper samples C before and after aging were as follow:

Before aging, The control sample of paper C (Fig. 2E) showed the presence of the OH stretching broad band at 3333 cm^{-1} (intensity 96.7), the C-H band at 2914 cm^{-1} and 2854 cm^{-1} (intensity 98.6 and 98.2, respectively), the C=O unconjugated band at 1726 cm^{-1} (intensity 99.4), the C=O conjugated and H-O-H bands at 1641 cm^{-1} (intensity 98.7), the CH_2-COH band of cellulose crystallization at 1421 cm^{-1} (intensity 98.8) and the C-O of cellulose polymerization at 1159, 1110, 1054, 1029 cm^{-1} and 1001 cm^{-1} (intensity 95, 93, 87, 89, 89, respectively). The control sample after aging (Fig. 2F) showed no changes in the intensity of the O-H stretching band at 3336 cm^{-1}, the C=O unconjugated band at 1725 cm^{-1}, the C=O conjugated band and the H-O-H band at 1640 cm^{-1}; however, an increase in the intensity of the CH_2-COH band is associated with the increase of amount of the crystalline structure of cellulose. An increase in the intensity of the C-O bands of cellulose polymerization at 1160, 1109, 1053, 1030 and 1000 cm^{-1} respectively was observed; this may be due to the re-polymerization which resulted from thermal aging.

Before aging, the samples treated with starch, SNPs dissolved in water, SNPs dissolved in acetone, SNPs dissolved in water blending with CMC, and SNPs dissolved in acetone blending with CMC showed an increase in the intensities of the bands of functional groups of tested consolidants (Fig. 2E). Post aging, a decrease in the intensities of the bands of functional groups was observed (Fig. 2F), But the sample treated with SNPs dissolved in acetone and SNPs dissolved in water blending with CMC gave no changes in the intensities of most studied bands. The sample treated with SNPs dissolved in acetone blending with CMC showed a slight increase in the intensity of the C-O bands of cellulose polymerization.

The results obtained (Fig. 2G and H) for the treated paper samples D before and after aging were as follow:

Before aging, The control sample of paper D (Fig. 2G) showed the presence of the O-H stretching broad band at 3339 cm^{-1} (intensity 94.2), the C-H band at 2894 cm^{-1} (intensity 97.4), the C=O unconjugated band at 1735 cm^{-1} (intensity 99.0), the C=O conjugated and H-O-H bands at 1640 cm^{-1} (intensity 98.3), the CH_2-COH band of cellulose crystallization at 1427 cm^{-1} (intensity 96.5) and C-O of cellulose polymerization at 1159, 1106, 1051 and 1026 cm^{-1} with intensity 92, 90, 84, 83, respectively. The control sample after aging (Fig. 2H) showed no change in the intensity of the O-H stretching band, the C=O conjugated band, and the H-O-H band. A decrease in the intensity of the C-O bands of cellulose polymerization at 1160, 1104, 1052 and 1025 cm^{-1} resulted from thermal aging.

The treated sample with starch before aging compared to the control sample (Fig. 2G) showed a

decrease in the intensity of the O-H stretching band at 3300 cm^{-1}, and a split of the C-H band at 2894 cm^{-1} into two bands at 2915 cm^{-1}, and 2873 cm^{-1}. A decrease in the intensity of the C-O bands of cellulose polymerization at 1155-1018 cm^{-1} was noticed; however, no change in the intensity of the C=O unconjugated band, the C=O conjugated band, the H-O-H band, and the CH_2-COH band of cellulose crystallization was observed. After aging (Fig. 2H), no change was observed except for an increase in the intensity of all C-O absorption bands of cellulose polymerization at 1155-900 cm^{-1}.

The treated sample with starch before aging compared to the control sample (Fig. 2G) showed a decrease in the intensity of the O-H stretching band at 3300 cm^{-1}, and a split of the C-H band at 2894 cm^{-1} into two bands at 2915 cm^{-1}, and 2873 cm^{-1}. A decrease in the intensity of the C-O bands of cellulose polymerization at 1155-1018 cm^{-1} was noticed; however, no change in the intensity of the C=O unconjugated band, the C=O conjugated band, the H-O-H band, and the CH_2-COH band of cellulose crystallization was observed. After aging (Fig. 2H), no change was observed except for an increase in the intensity of all C-O absorption bands of cellulose polymerization at 1155-900 cm^{-1}.

The samples treated with SNPs dissolved in water, SNPs dissolved in acetone, SNPs dissolved in acetone blending with CMC, and SNPs dissolved in water blending with CMC showed an increase before aging and a decrease after aging in the bands intensities of the studied functional groups (Fig. 2G). After aging (Fig. 2H), the treated sample showed no change except for a decrease in the band intensity of the CH_2-COH band of cellulose crystallization , and an increase in the intensity of all C-O bands of cellulose polymerization at 1061-1025 cm^{-1}.

3.5. Investigation of the surface morphology by scanning electron microscope

For this procedure, only the most effective polymer for each type of paper was selected based on the results of the previous analytical techniques with the aim of investigating the surface morphology of each selected sample.

3.5.1. Investigation of the surface morphology of the tracing paper A

The results (Fig. 3A) showed that the aged control sample is made of cotton fibers and appear with a semi-regular distribution. Some gaps are found in the paper surface. The fibers became rough as a result of thermal aging. Damage was also noticed for some fibers. The unaged sample treated with starch nanoparticles dissolved in water (Fig. 3B) showed good coating for the polymer on the surface. The fiber distribution was good. The smoothness of the fibers was also good. Results were approximately the same after aging (Fig. 3C) with the samples showing good coating and good fiber distribution. The unaged paper A treated with starch nanoparticles dissolved in acetone (Fig. 3D) showed good coating as well; however, it did not fully penetrate through the fiber structure; and this may be due to the speed of acetone evaporation. Some gaps are also found on the surface; and this may due to the non-homogenous structure of the paper. The aged sample (Fig. 3E) showed good coating and good fibers distribution. Some gaps are also noticed on the paper surface.

3.5.2. Investigation of the surface morphology of the tracing paper B

For the aged control sample (Fig. 4A), the presence of discontinuous fibers, lack of homogeneity of the fibrous structure, and roughness were noticed. This may due to the effect of sulfuric acid used in the preparation of the paper sample. For the unaged paper treated with starch nanoparticles dissolved in water blending with CMC (Fig. 4B), it is obvious that the consolidant material improved the condition of the fibers, which appeared strong; however, the fiber structure slightly disappeared. For the same sample after aging (Fig. 4C), accelerated thermal aging slightly affected the fibers, which nevertheless are still strong. It was also noticed that the consolidation material does not remain condensed on the surface compared to the sample before aging. The unaged sample treated with starch dissolved in water (Fig. 4D) showed good distribution for the consolidant, and the fiber appeared in a good state. For the same sample after aging (Fig. 4E), thermal aging affected the fibers which appeared stiff and a lack of coverage for the consolidant material on the surface was noticed.

3.5.3. Investigation of the surface morphology of the tracing paper C

The aged control sample (Fig. 5A) showed erosion of some fibers, roughness of the fibers, and some gaps were also observed. These results indicate the effect of thermal aging on the sample without treatment.

The unaged sample treated with starch nanoparticles dissolved in water with the addition of CMC (Fig. 5B) showed good distribution of the consolidation material on the surface; however, the fiber structure disappeared in some area; and this may due to the abundant presence of consolidation material in some area. The same sample after aging (Fig. 5C) clearly showed the fiber structure and exhibited a slight roughness of the fibers. The unaged sample treated with starch dissolved in water (Fig. 5D) showed a good distribution of the consolidant used, the fibers became strong, and some gaps were

Table 3

Change of color of treated different tracing paper with different consolidants before and after heat ageing

Color values/ total color differences	Treated different tracing paper before ageing																							
	Impregnated paper (A)						Vegetable parchment paper (B)						Vegetable parchment paper (C)						Modern tracing paper (D)					
	CS	1A	2A	3A	4A	5A	CS	1B	2B	3B	4B	5B	CS	1C	2C	3C	4C	5C	CS	1D	2D	3D	4D	5D
L*	84.90	82.15	82.57	84.68	83.89	82.43	95.16	94.44	94.52	93.83	91.77	93.07	94.55	93.86	94.01	93.94	93.29	93.79	75.36	79.35	81.64	80.38	76.23	76.75
a*	-2.49	-2.55	-2.73	-2.56	-1.74	-2.47	-0.79	-0.32	-0.51	-0.51	-0.73	-0.68	-0.18	-0.46	-0.56	0.67-	-0.60	-0.65	-0.69	-0.63	-0.75	-0.62	-0.69	-0.54
b*	10.91	10.39	12.92	14.55	13.41	12.93	5.43	1.96	3.89	3.47	3.49	4.86	2.00	2.12	2.87	3.20	3.68	3.19	0.71	1.75	2.45	2.14	3.25	2.56
ΔE	0.00	2.01	2.53	2.69	2.62	2.61	0.00	1.83	2.84	2.43	2.83	3.56	0.00	0.75	1.09	1.43	2.14	1.49	0.00	2.31	3.48	3.31	2.63	2.03
	Treated different tracing paper after ageing																							
Color values/ total color differences	Impregnated paper (A)						Vegetable parchment paper (B)						Vegetable parchment paper (C)						Modern tracing paper (D)					
	CS	1A	2A	3A	4A	5A	CS	1B	2B	3B	4B	5B	CS	1C	2C	3C	4C	5C	CS	1D	2D	3D	4D	5D
L*	80.64	83.10	82.89	84.44	77.63	78.15	91.74	93.26	92.48	92.73	92.32	92.27	93.99	93.89	93.76	93.39	92.49	92.68	74.57	77.42	78.37	78.34	76.03	76.19
a*	-0.77	-0.59	-0.79	-1.26	3.11	2.64	-0.42	-0.38	-0.52	-0.41	-0.54	-0.55	-0.21	-0.41	-0.42	0.25-	-0.69	-0.72	-0.39	-0.57	-0.43	-0.35	-0.64	-0.57
b*	24.52	25.09	24.34	22.19	27.44	27.62	2.27	3.09	4.28	5.27	7.39	3.86	2.35	5.05	4.34	5.92	5.44	5.60	2.99	4.84	5.95	6.21	5.05	4.88
ΔE	0.00	2.53	2.29	2.52	5.71	5.24	0.00	1.09	2.11	2.28	2.63	6.14	0.00	0.99	2.01	2.62	2.47	2.58	0.00	5.13	7.66	6.64	2.66	2.89

Table 4

Measurement of pH values of tracing paper (A, B, C and D) treated with Consolidants before and after accelerated heat ageing

	Paper A		Paper B		Paper C		Paper D	
C.	**B.A.**	**A.A.**	**B.A.**	**A.A.**	**B.A.**	**A.A.**	**B.A.**	**A.A**
C.S.	6.2	6.0	7.0	7.0	7.0	6.5	7.0	6.8
1	6.2	6.0	7.0	6.8	6.8	6.5	6.9	6.7
2	6.5	6.0	6.8	6.3	7.0	6.8	7.0	6.8
3	6.3	6.1	6.5	6.4	7.0	6.7	6.9	6.7
4	7.0	6.7	6.7	6.3	6.9	6.3	7.1	7.0
5	7.0	6.8	6.8	6.5	7.0	6.7	7.3	7.0

C. = Consolidants, B. A. = Before ageing, A.A. = After ageing

also observed which may due to the manufacturing process. The same sample after aging (Fig. 5E) showed the effect of thermal aging on the sample since some fibers appeared to be eroded despite that other fibers appeared well covered with consolidant.

3.5.4. Investigation of the surface morphology of the tracing paper D

The aged control sample (Fig. 6A) showed damage and roughness of some fibers and gaps. On the other hand, the sample treated with starch nanoparticles dissolved in acetone with the addition of CMC (Fig. 6B) showed good results in term of surface morphology, which appeared smooth and strong. The same sample after aging (Fig. 6C) showed good distribution for the consolidation material on the surface compared to the same sample before aging. The sample treated with starch nanoparticles dissolved in acetone (Fig. 6D) gave good penetration through the fiber structure, good distribution on the surface, and the surface became smooth and clear. The same sample after aging (Fig. 6E) showed roughness of the surface as a result of thermal accelerated aging.

4. Conclusion

The results of mechanical properties (tensile strength and elongation), measurement of color and SEM proved that starch nanoparticles dissolved in water or acetone, starch nanoparticles dissolved in water or acetone blending with CMCb gave an effectiveness in the improvement of tracing paper especially for the types A, B and C.

The results stated that the tracing paper D is sensitive to aqueous treatments. Sight changes in pH value were noticed for the paper samples treated with consolidants before and after the aging process. FTIR analysis proved that all changes in the functional groups and chemical composition of aged treated samples A, B, C, and D were limited to a slight decrease in the moisture of the paper, a decrease in intensity of cellulose crystallization absorption bands, and change in the intensity of the absorption bands of cellulose polymerization. All previous changes are normal results of the effect of thermal aging on cellulose. The analytical techniques used proved that the best results were obtained by using starch nanoparticles dissolved in water for paper A, starch nanoparticles dissolved in water blending with CMC for paper B and C, and starch nanoparticles dissolved in acetone followed by starch nanoparticles dissolved in acetone blending with CMC for paper D.

References:

1. Axelsson K, (2016) Transparent papers: A review of the history and manufacturing processes, IPH Paper History. 20: 21-31.
2. Laroque C (2004) History and analysis of transparent papers, Pap. Conserv. 28: 17-32.
3. Page S (1997) Conservation of Nineteenth–century tracing paper, a quick practical Approach, BPG Annual. 16: 67-73.
4. Van der Reyden D, Hofmann C, Baker M (1993) Effect of aging and solvent treatments on some properties of contemporary tracing papers, JAIC.32: 177-206.
5. Homburger H, Korbel B (1999) Architectural drawings on transparent paper: modification of conservation treatments, BPG Annual.18: 25-33.
6. Wilson H (2015) A decision frame work for the preservation of transparent papers, J. Inst. Conserv.38: 2-3. http://dx.doi.org/10.1080/19455224.2014.999005
7. Lubick A (1999) Architectural Drawings, CRM. 22(7): 40-41.
8. Giedraitiene B, Steponaviciute M (2019) Analysis of works on tracing paper from a collection of drawings by Lithuanian artists. In: Golob N, Tomažič J (ed) Works of Art on parchment and paper Interdisciplinary Approaches, Ljubljana University Press, Ljbljana, pp.173-176 .https://doi.org/10.4312/9789610602743

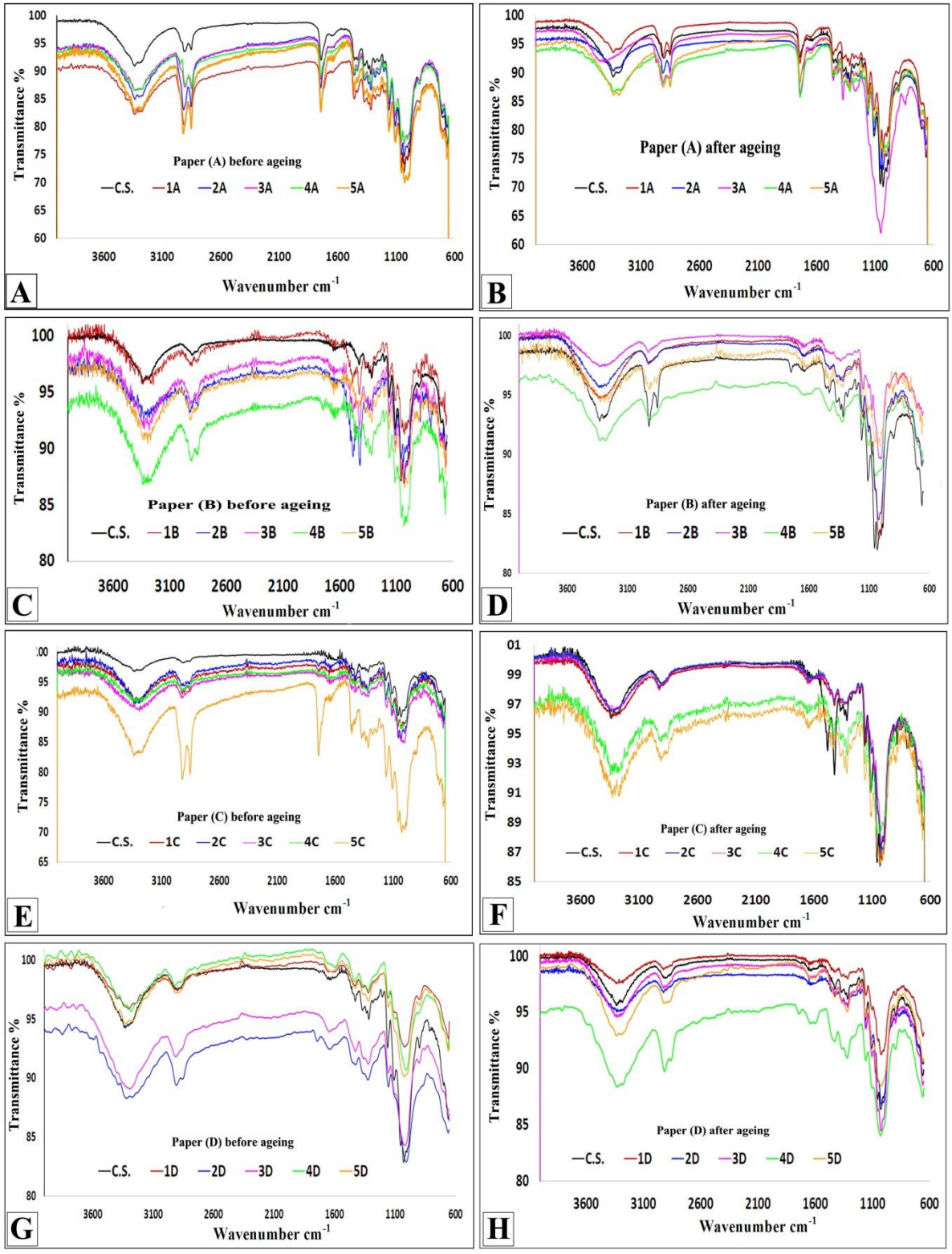

Fig. 2. ATR-FTIR analysis of treated tracing papers with different consolidants before and after aging: (A, B) Tracing paper A, (C, D) Tracing paper B, (E, F) Tracing paper C, (G, H) Tracing paper D.

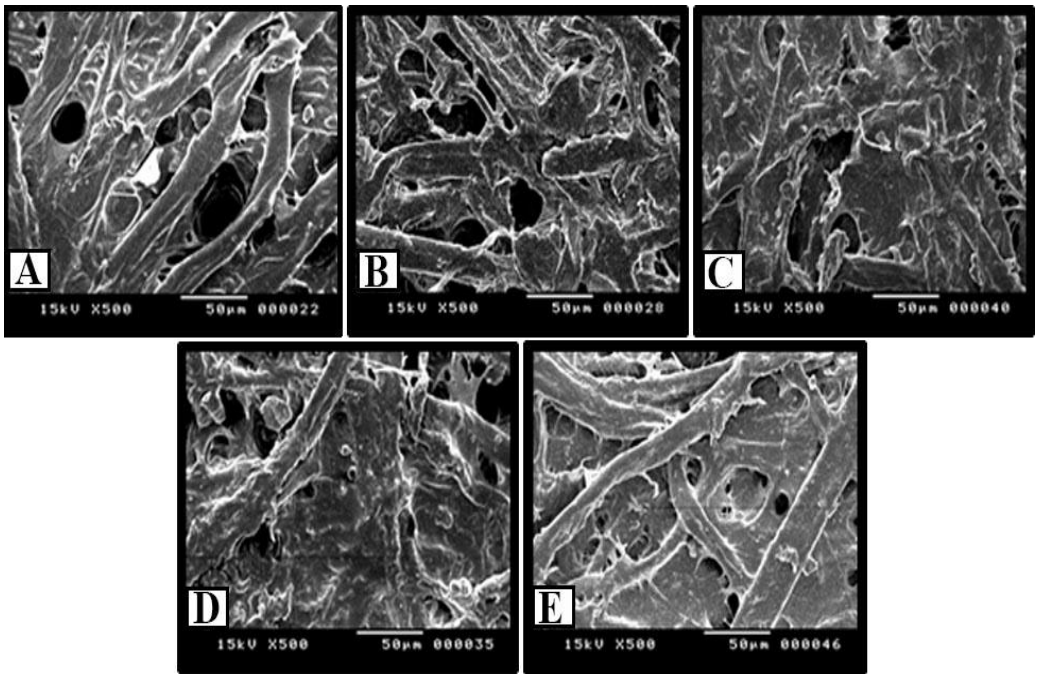

Fig. 3. SEM micrographs for consolidated tracing paper A: (A) Aged sample without treatment (control sample), (B) Treated paper with SNPs dissolved in water before ageing, (C) Treated paper with SNPs dissolved in water after ageing, (D) Treated paper with SNPs dissolved in acetone before ageing, (E) Treated paper with SNPs dissolved in acetone after ageing.

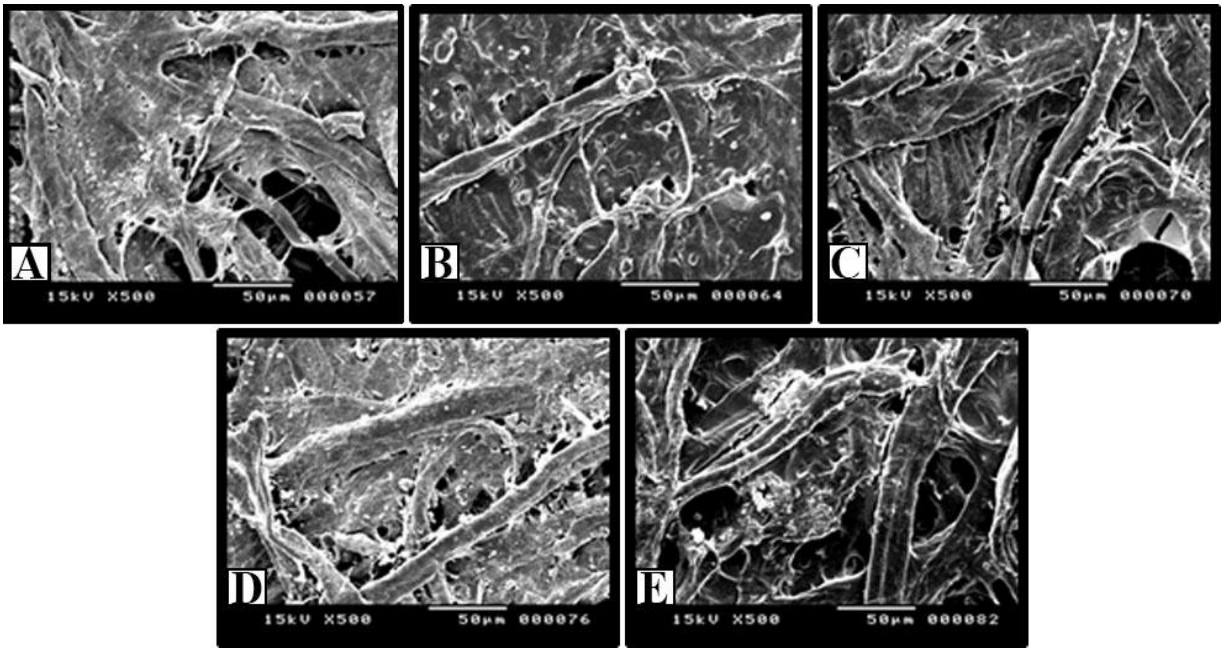

Fig. 4. SEM micrographs for consolidated tracing paper B: (A) Aged sample without treatment (control sample), (B) Treated paper with starch nanoparticles dissolved in water with addition of CMC before ageing, (C) Treated paper with starch nanoparticles dissolved in water with addition of CMC after ageing, (D) Treated paper with starch dissolved in water before ageing, (E) Treated paper with starch dissolved in water after ageing.

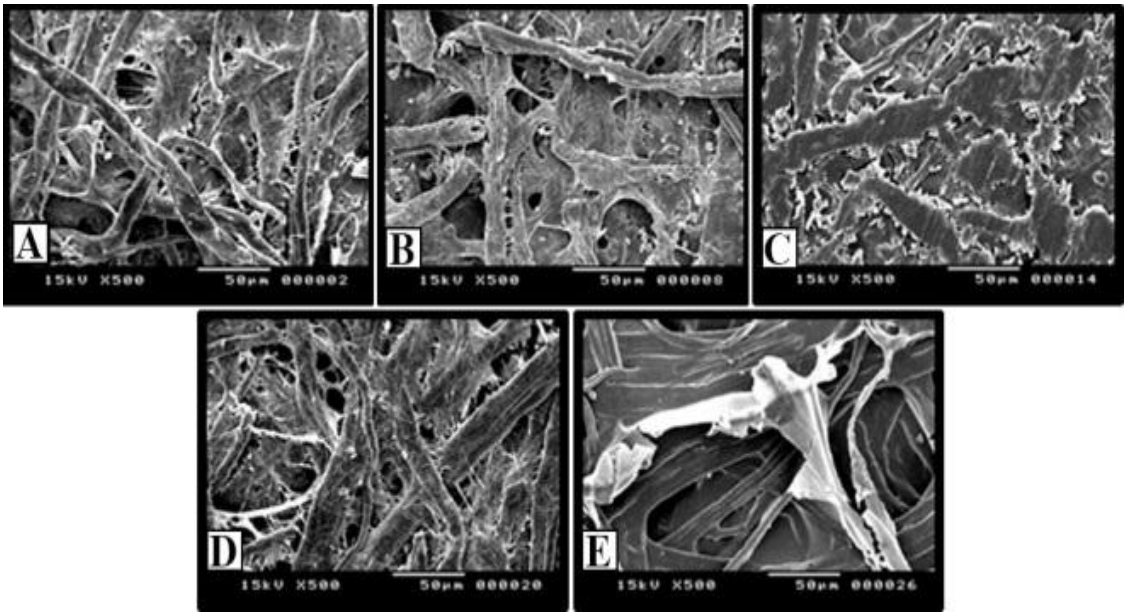

Fig. 5. SEM micrographs for consolidated tracing paper C: (A) Aged sample without treatment (control sample), (B) Treated paper with starch nanoparticles dissolved in water with addition of CMC before ageing, (C) Treated paper with starch nanoparticles dissolved in water with addition of CMC after ageing, (D) Treated paper with starch dissolved in water before ageing, (E) Treated paper with starch dissolved in water after ageing

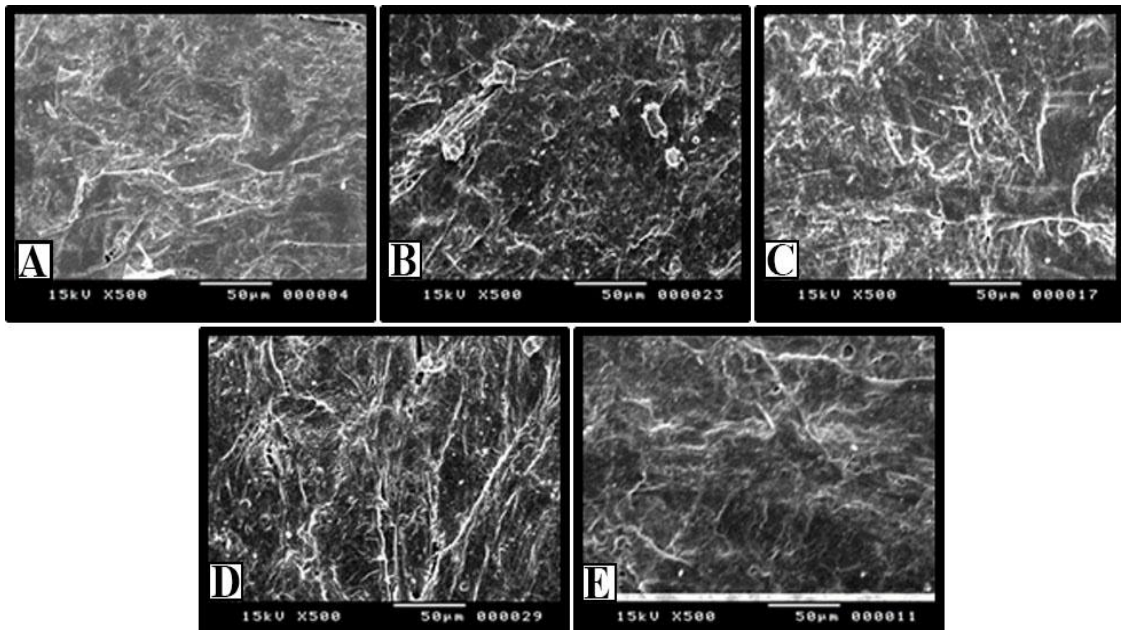

Fig. 6. SEM micrographs for consolidated tracing paper D: (A) Aged sample without treatment (control sample), (B) Treated paper with starch nanoparticles dissolved in acetone with addition of CMC before ageing, (C) Treated paper with starch nanoparticles dissolved in acetone with addition of CMC after ageing, (D) Treated paper with nano starch dissolved in acetone before ageing, (E) Treated paper with nano starch dissolved in acetone after ageing

9. Cook P, Dennin J (1994) Ships plans on oil and resin impregnated tracing paper: a practical repair procedure, Pap. Conserv. 18: pp.11-9. https://doi.org/10.1080/03094227.1994.9638584
10. Bachmann K (1983) Treatment of Transparent Papers: a Review, BPG Annual.2: 3-14.
11. Van der Reyden D, Hofmann C, Baker M, Mecklenburg M (1992) Modern Transparent Papers: Materials, Degradation, and the Effects of Some Common Treatments. In: Vandiver P, James D, Wheeler G, Freestone I (ed) Materials Issues in Art and Archaeology III, Materials Research Society, Pittsburgh, Pennsylvania, pp. 379–395. https://doi.org/10.1557/PROC-267-379
12. Santos A (17-19 April 2013) Preservation of Architectural Drawings on Translucent paper in Brazil: Conservation Methods in public Institutions, In: Hofmann C, Watteeuw L (ed) Paper conservation: Decisions & Compromises, ICOM-CC Graphic Document Working Group Interim Meeting Vienna, Austrian National Library, p.66.
13. Juranic S, zavod H (2015) Kinds of damages and conservation and restoration methods in restoration of works of art on the transparent paper, Vjesn. Bibl. Hrvat.58 (3).
14. Suligoj T (2019) Technical Drawings: conservation treatment, In: Golob N, Tomažič J (ed) Works of Art on parchment and paper Interdisciplinary Approaches, Ljubljana University Press, Ljbljana, pp.177-180. https://doi.org/10.4312/9789610602743
15. Ardelean E, Nicu R, Asandei D, Bobu E (2009) Carboxymethy- Chetosan as consolidation agent for old documents on paper support, Eur. J. Sci. Theol.5(4): 67-75.
16. Wasiutynski T (1980) Sprayed poly (vinyl acetate) heat seal adhesive lining of pen and iron ink drawings on tracing paper, JAIC.19(2): 96-102.
17. Yates S (1984) Conservation of Nineteenth - century tracing paper, Pap. Conserv. 8(1): 20-39. https://doi.org/10.1080/03094227.1984.9638456
18. Greuter E (2019) The value of conservation and digitization of architectural and design drawings for historical research, In: Golob N, Tomažič J (ed) Works of Art on parchment and paper Interdisciplinary Approaches, Ljubljana University Press, Ljbljana, pp. 151- 158. https://doi.org/10.4312/9789610602743
19. Bicchieri M, Brusa P, Pasquariello G (1993) Tracing paper: Methods of study and restoration, Restaurator. 14(4): 217-233.
20. Wanser H (2001) Conservation corner preserving Lafayette's 1824 Maps, Library of Congress Information Bulletin. 60(4).
21. Saada N, Abdel-Maksoud G, Abd El-Aziz M, Youssef A (2021) Green synthesis of silver nanoparticles, characterization, and use for sustainable preservation of historical parchment against microbial biodegradation, Biocatalysis and Agricultural Biotechnology, 32: 101948, https://doi.org/10.1016/j.bcab.2021.101948.
22. Sun Q, Li G, Lei D, Ji N, Xiong L (2014) Green preparation and characterization of waxy maize starch nanoparticles through enzymolysis and recrystallization, Food Chem.162: 223-228.
23. Silva N, Lima F, Fialho R, Albuquerque E, Velasco J, Fakhouri F (2018) Production and Characterization of Starch Nanoparticles, In Huicochea E, Rendon R (ed) Application of modified starches, Intechopen Limited, London, United Kingdom, , pp. 41-48.
24. Aldao D, Sarka E, Ulbrich P, Mensikove E (2018) Starch Nanoparticles –Two Ways of their preparation, Czech J. Food Sci. 36(2): 133–138.
25. Lin N, Huang J., Chang P., Anderson D., Yu J. (2011) Preparation, Modification, and Application of Starch Nanocrystals in Nanomaterials: A Review, J. Nanomater. 2011: 573687. https://doi.org/10.1155/2011/573687
26. Teygeler R (2004) Preserving Paper: Recent Advances, In Feather J (ed) Managing preservation for libraries and archives, Current practice and future developments, 1st edition, Routledge, London, pp.83-112. https://doi.org/10.4324/9781315249919
27. Feller R (1994) Accelerated Aging Photochemical and Thermal Aspects, In Berland D (ed) Research in Conservation, The Getty Conservation Institute, U.S.A., P.1.
28. Zervos S, Moropoulou A (2006) Methodology and Criteria for the Evaluation of Paper Conservation Interventions: A Literature Review, Restaurator. 27(4): 219–274.
29. Ahmed H, Mohamed W, Saad H, Nasr H, Morsy M, Mahmoud N (2017) Degradation Behavior of Nano-Glue Adhesive due to Historical Textiles Conservation Process, Egypt. J. Chem. 60(6): 1-12.
30. Bajpai P (2018) Biermann's Handbook of Pulp and Paper, Vol. 2: Paper and Board Making, 3th Edition, Elsevier, pp. 35-63. https://doi.org/10.1016/C2017-0-00513-X
31. Abdel-Maksoud G, Emam H, Ragab N (2020) From traditional to laser cleaning techniques of parchment manuscripts: A review, ARCS. 1(1): 69-70.
32. Abdel-Maksoud G, Sobh R, Tarek A, Radwan S (2019) Evaluation of montmorillonite (MMT)/polymer nanocomposite in gap filling of archaeological bones, Egypt. J. Chem. 63(5): 1585 – 1603.
33. Abdel–Aty Y, Mahmoud H, Al-Zahrani A (2020) Experimental evaluation of consolidation techniques of fossiliferous limestone in masonry

walls of heritage buildings at historic Jeddah, Kingdom of Saudi Arabia, ARCS.1(1): 16-33.
34. Hamed S, El Hadidi N (2020) The Use of SEM-EDX investigations in estimating the penetration depth of preparation layers within wood structure, ARCS.1 (1): 1-15.
35. Helmi F, Hefni Y (2020) Estimation of deterioration aspects of granitic columns at the Mosque of Al-Nasir Mohamed Ibn Qalawun, Cairo, Egypt, ARCS.1 (1): 34- 51.
36. Abdel-Maksoud G, Abdel-Hamied M, El-Shemy H (2021) Analytical techniques used for condition assessment of a late period mummy, J. Cult. Herit. 48: 83-92 https://doi.org/10.1016/j.culher.2021.01.001
37. Cocca M, D'Arienzo L, D'Orazio L (2011) Effects of Different Artificial Aging on Structure and Properties of Whatman Paper Samples, ISRN Materials Science. 2011: 1- 7.
38. Jinxia M, Zhiguo W, Xiaofan Z, Huining X (2015) Self-Reinforced Grease-Resistant Sheets Produced by Paper Treatment with Zinc Chloride Solution, BioRes.10(4): 8225- 8237.
39. Duan B, Sun P, Wang X, Yang C (2011) Preparation and properties of starch nanocrystals / carboxymethyl chitosan nanocomposite films, Starch.63(9): 528-535.
40. Ghanbarzadeh B, Almasi H, Entezami A (2010) Physical properties of edible modified starch/carboxymethyl cellulose films, IFSET.11 (4): 697-702. https://doi.org/10.1016/j.ifset.2010.06.001
41. Tongdeesoontorn W, Mauer L, Wongruong S, Sriburi P, Rachtanapun P (2011) Effect of carboxymethyl cellulose concentration on physical properties of biodegradable cassava starch-based films, Chem. Cent. J.5 (6).
42. Qiao Z, Gu J, Zuo Y, Tan H, Zhang Y (2014) The Effect of Carboxymethyl Cellulose Addition on the Properties of Starch-based Wood Adhesive, BioRes. 9 (4): 6117- 6129.
43. Mandal A, Chakrabarty D (2018) Studies on mechanical, thermal, and barrier properties of carboxymethyl cellulose film highly filled with nanocellulose, J. Thermoplast. Compos. Mater. 32 (7): 995-1014.
44. Jannatyha N, Shojaee- Aliabadi S, Moslehishad M, Moradi E (2020) Comparing mechanical, barrier and antimicrobial properties of nanocellulose/CMC and nanochitosan/CMC composite films, Int. J. Biol. Macromol.164: 2323-2328.
45. Bora D, Gupta A, Khan F (2015) Comparing the Performance of L*a*b* and HSV Color Spaces with Respect to Color Image Segmentation, IJETAE. 5(2): 194-195.
46. Szucs V, Lanyi C (2017) Online colour representation of museum artefacts, In Best J (ed) Colour Design, Theories and Applications, 2nd edition, Woodhead publishing, Elsevier, pp. 641-651.
47. Nilsen C (1996) Managing the Analytical Laboratory, plain and simple, 1st edition, CRC Press, U.S.A., P.83.
48. Harrigan W (1998) Laboratory Methods in food Microbiology, 3th edition, Academic Press Limited, U.S.A., p.80.
49. May E, Jones M (2006) Conservation Science: Heritage Materials, RSCP Publishing, Cambridge, England, P.53.
50. Fouda A, Abdel-Maksoud G, Saad H, Gobouri A, Mohammedsaleh Z, El-Sadany M (2021) The Efficacy of Silver Nitrate (AgNO3) as a Coating Agent to Protect Paper against High Deteriorating Microbes, Catalysts.11(310).
51. Kim H (2012) Scientific Examination and Analysis of paper cultural properties, In Conservation of paper and textiles, National Research Institute of Cultural Heritage, Korea, p.246.
52. Shahani C (November 1995) Accelerated Aging of Paper: Can It Really Foretell the Permanence of Paper, Preservation Research and Testing Series, Library of Congress.9503:1-18.
53. Considine J, Hotle B, Wald M, Rowlands R, Turner K (2-5 June 2008) Effects of thermal aging on mechanical performance of paper, Proceedings: Progress in Paper Physics Seminar, Helsinki University of Technology (TKK), Espoo, Finland, pp. 271-273.
54. Zhu M, Chen Y, Gu C, Zhu W, Ma X, Wang X (2017) Effect of Thermal Aging on the Properties of Insulating Paper, Advances in Engineering Research Series.146:122-125. https://doi.org/10.2991/icmea-17.2018.28
55. Chapdelaine P, Arney J (1982) A kinetic study of the influence of acidity on the accelerated aging of paper, JAIC. 22(1): 25- 36.
56. Zou X, Gurnagul N, Uesaka T, Bouchard J (1994) Accelerated aging of papers of pure cellulose: mechanism of cellulose degradation and paper embrittlement, Polym Degrad Stab. 43(3): 393-402. https://doi.org/10.1016/0141-3910(94)90011-6
57. Whitmore P, Bogaard J (1995) The effect of oxidation on the subsequent oven aging of filter paper, Restaurator. 16 (1): 10-30.
58. Barański A, Konieczna-Molenda A, Łagan J, Proniewicz L (2003) Catastrophic room temperature degradation of cotton cellulose, Restaurator. 24(1): 36-45.

59. Chandra K, Visakh M, Thomas S, Mathew P (2013) Advances elastomers II: composites andNanocomposites, Spinger International Publishing, Berlin, p.77.
60. Dufresne A (2015) Starch and Nanoparticle, Springer International Publishing, Switzerland, pp.417-447.
61. Liu C, Jiang S, Zhang S, Xi T, Sun Q, Xiong L (2016) Characterization of edible corn starch nanocomposite films: The effect of self-assembled starch nanoparticle, Starch. 68(3): 239–248. https://doi.org/10.1002/star.201500252
62. Sandhu K, Nian V (2017) Starch Nanoparticles: Their Preparation and Applications, In Gahlawat S, Salar R, Siwach P, Duhan J, Kumar S, Kaur P (ed) Plant Biotechnology: Recent Advancements and Developments, Spinger press, pp. 213-232.
63. Huicochea E, Rendon R (2018) Applications of Modified Starches, IntechOpen, London, United Kingdom, , p. 45.
64. Zervos S (2010) Natural and Accelerated Ageing of Cellulose and Paper: A literature review, In Lejeune A, Deprez T (ed) Cellulose, Structure and Properties, Derivatives and Industrial Uses, Nova Publishing, pp. 155-203.
65. Ardelean E, Bobu E, Niculescu G, Groza C (2011) Effects of different consolidants additives on ageing behavior of archived document paper, Cellul. Chem. Technol.45 (1):.97-103.
66. Karlovits M, Gregor-Svetec D (2012) Durability of Cellulose and Synthetic Papers Exposed to Various Methods of Accelerated Ageing, Acta Polytech. Hungarica. 9 (6): 82-100.
67. Gonçalves P, Brandelli A, Noreña C, Silveira N (2014) Characterization of starch nanoparticles obtained from Araucaria angustifolia seeds by acid hydrolysis and ultrasound, LWT. 58 (1): 21-27.
68. Asl S, Mousavi M, Labbafi M (2017) Synthesis and Characterization of Carboxymethyl Cellulose from Sugarcane Bagasse, J Food Process Technol. 8 (8).
69. Rosenau T, Potthast A, Hell J (2019) Cellulose Science and Technology, Chemistry, Analysis, and Applications, WILEY, Vienna, p.176.
70. Ardelean E (2007) Study on Some Resizing and Consolidation Methods of Old Paper, Eur. J. Sci. Theol.3 (3): 53-61.
71. Area M, Cheradame H (2011) Paper aging and degradation, Recent findings and research methods, BioRes. 6(4): 5307-5337.
72. Ahn K, Zaccaron S, Zwirchmayr N, Hettegger H, Hofinger A, Bacher M, Henniges U, Hosoya T, Potthast A, Rosenau T (2019) Yellowing and brightness reversion of celluloses: CO or COOH, who is the culprit?, Cellulose. 26 (1): 429–444. https://doi.org/10.1007/s10570-018-2200-x.
73. Fan M, Dai D, Huang B (2012) Fourier Transform Infrared Spectroscopy for Natural Fibers, In Salih S (ed) Fourier Transform – Materials Analysis, Intech open, pp.46-70.
74. Wulandari W, Rochliadi A, Arcana M (2016) Nanocellulose prepared by acid hydrolysis of isolated cellulose from sugarcane bagasse, IOP Conf. Ser.: Mater. Sci. Eng.107.
75. Hospodarova V, Singovszka E, Stevulova N (2018) Characterization of cellulosic fibers by FTIR Spectroscopy For their further implementation to building materials, American Journal of Analytical Chemistry. 9(6):303-310.
76. Galiwango E, Abdel Rahman N, Al-Marzouqi A, Abu-Omar M, Khaleel A (2019) Isolation and characterization of cellulose and α – cellulose from date palm biomass waste, Heliyon. 5 (12). https://doi.org/10.1016/j.heliyon.2019.e02937
77. Łojewska J, Miśkowiec P, Łojewski T, Proniewicz L (2005) Cellulose oxidation and hydrolytic degradation: In situ FTIR approach, Polym. Degrad. Stab. 88 (3): 512-520.
78. Darwish S, El Hadidi N (4-6 March 2008) The Effect of Solvents on the Chemical Composition Of Archaeological Wood, International Conference on Giza through the Ages, Faculty of Archaeology, Cairo University, Egypt, pp.1-17.
79. Munajed A, Subroto C, Suwarno S (2018) Fourier Transform Infrared (FTIR) Spectroscopy Analysis of Transformer paper in Mineral Oil-paper composite Insulation under Accelerated Thermal Aging, Energies.11 (2) :364. https://doi.org/10.3390/en11020364
80. Rantuch P, Chrebet T (2014) Thermal Decomposition of Cellulose Insulation, Cellulose Chem. Technol. 48(5): 461-467.
81. Jusner P, Schwaiger E, Potthast A, Rosenau T (January 2021) Thermal stability of cellulose insulation in electrical power transformers – A review, Carbohydr. Polym.252: 117196.
82. Olsson M, Salmen L (2004) The association of water to cellulose and hemicellulose in paper examined by FTIR spectroscopy, Carbohydr. Res. 339 (4): 813-818.
83. Mends J, Paschoalin R, Carmona V, Neto A, Marques A, Marconcini J, Mattoso L, Medeiros E, Oliveira J (2016) Biodegradable polymer blends based on corn starch and thermoplastic chitosan processed by extrusion, Carbohydr. Polym. 137: 452- 458.
84. Safari J, Aftabi P, Ahmadzadeh M, Sadeghi M, Zarnegar Z (2017) Sulfonated starch nanoparticles: An effective, heterogeneous and bio-based catalyst for synthesis of 14-aryl-14- H – dibenzo [a,j] xanthenes, J. Mol. Struct.1142: 33-39. https://doi.org/10.1016/j.molstruc.2017.02.095Get

85. Liu C, Li M, Ji N, Liu J, Xiong L, Sun Q (2017) Morphology and Characteristics of Starch Nanoparticles Self-Assembled via a Rapid Ultrasonication Method for Peppermint Oil Encapsulation, J Agr Food Chem 65(38): 8363–8373. https://doi.org/10.1021/acs.jafc.7b02938
86. Guo X, Wu Y, Yan N (2017) Characterizing spatial distribution of the adsorbed water in wood cell wall of Ginkgo biloba L. by μ-FTIR and confocal Raman spectroscopy, Holzforschung.71(5): 415-423. https://doi.org/10.1515/hf-2016-0145
87. Capanemaa N, Mansur A, Jesus A, Carvalho S, Oliveira L, Mansur H (2018) Superabsorbent crosslinked carboxymethyl cellulose-PEG hydrogels for potential wound dressing applications, Int. J. Biol. Macromol.106: 1218-1234. https://doi.org/10.1016/j.ijbiomac.2017.08.124
88. Lan W, He L, Liu Y (2018) Preparation and Properties of Sodium Carboxymethyl Cellulose/Sodium Alginate/Chitosan Composite Film, Coatings. 8(8): 291. https://doi.org/10.3390/coatings8080291
89. Guo X, Liu L, Wu J, Fan J, Wu Y (2018) Qualitatively and quantitatively characterizing water adsorption of a cellulose nanofiber film using micro-FTIR spectroscopy, RSC Adv.8:4214- 4220.
90. Cortes U, González-Cruz L, Velazquez G, Teniente-Martínez G, Gómez-Aldapa C, Castro-Rosas J (2019) Bernardino-Nicanor A, Effect of Dual Modification on the Spectroscopic, Calorimetric, Viscosimetric and Morphological Characteristics of Corn Starch, Polymers, MDIP, Vol. 11(2): 333.
91. Cichosz S, Masek A (2020) IR on cellulose with the varied moisture contents: insight into the supramolecular structure, Materials. 13(20): 4573. https://doi.org/10.3390/ma13204573
92. Gorassini A, Calvini P, Baldin A (1-4 June 2008) Fourier Transform Infrared Spectroscopy (FTIR) analysis of historic paper documents as a preliminary step for chemo metrical analysis, CMA4CH 2008, Mediterraneum Meeting, Multivariate Analysis and Chemometrics Applied to Environment and Cultural Heritage, 2nd ed., Ventotene Island, Italy, Europe.
93. Traore M, Kaal J, Cortizas A (2016) Application of FTIR spectroscopy to the characterization of archeological wood, SAA. 153:63-70. https://doi.org/10.1016/j.saa.2015.07.108
94. Yang Y, Zhang Y, Lang Y, Yu M (2017) Structural ATR-IR analysis of cellulose fibers prepared from a NaOH complex aqueous solution, IOP Conf. Ser.: Mater. Sci. Eng. 213:012039
95. Ferrer N, Sistach C (2007) FTIR Technique used to study Acidic paper manuscripts dating from the thirteenth to sixteenth century from archive of the crown of Aragon, BPG Annual .26: 21-25.
96. Łojewski T, Miśkowiec P, Missori M, Lubańska A, Proniewicz L, Łojewska J (2010) FTIR and UV/ Vis as methods for evaluation of oxidative degradation of model paper: DFT approach for carbonyl vibrations, Carbohydr. Polym.82 (2): 370 -375. https://doi.org/10.1016/j.carbpol.2010.04.087
97. Librando V, Minniti Z (2011) Ancient and modern paper characterization by FTIR and MICRO-RAMAN spectroscopy, Conservation Science in Culture Heritage. 11(1): 249- 268. https://doi.org/10.6092/issn.1973-9494/2700